*Int. J. Therm. Sci.* (2000) 39, 582–591

S1290-0729(00)00207-6/FLA

# Characterisation of the spray cooling heat transfer involved in a high pressure die casting process

Guang Wei Liu [a*], Yosry Sadeik Morsi [a], Brian Robert Clayton [b]

[a] *Center for Modelling and Process Analysis, School of Engineering and Science, Swinburne University of Technology, John Street, Hawthorn, P.O. Box 218, Victoria 3122, Australia*

[b] *School of Mechanical, Materials, Manufacturing Engineering and Management, University of Nottingham, University Park, Nottingham, NG7 2RD, UK*

(Received 22 June 1999, accepted 4 October 1999)

**Abstract**—A systematic experimental study was conducted to examine the heat transfer characteristics from the hot die surface to the water spray involved in high pressure die casting processes. Temperature and heat flux measurements were made locally in the spray field using a heater made from die material H-13 steel and with a surface diameter of 10 mm. The spray cooling curve was determined in the nucleate boiling, critical heat flux, as well as the transition boiling regimes. The hydrodynamic parameters of the spray such as droplet diameters, droplet velocities, and volumetric spray flux were also measured at the position in the spray field identical to that of the test piece. Droplet size and velocity distribution were measured using a PDA system. A new empirical correlation was developed to relate the spray cooling heat flux to the spray hydrodynamic parameters such as liquid volumetric flux, droplet size, and droplet velocity in all heat transfer regimes. The agreement between experimental data and predicted results is satisfactorily good. © 2000 Éditions scientifiques et médicales Elsevier SAS

**spray cooling / surface heat flux / droplet velocity / droplet diameter / high pressure die casting**

## Nomenclature

| | | |
|---|---|---|
| $A_1, A_2, \ldots, A_5$ | areas | $m^2$ |
| $A, B, C, D$ | coefficients in equation (5) | |
| $C_{pl}$ | liquid specific heat | $J \cdot kg^{-1} \cdot K^{-1}$ |
| $D_{32}$ | Sauter mean diameter | m |
| $d_0, d_1, \ldots, d_5$ | droplet Sauter mean diameter at locations 0 to 5 shown in *figure 4* | m |
| $\overline{d}$ | cross-surface Sauter mean diameter | m |
| $h_{fg}$ | latent heat of vaporization | $J \cdot kg^{-1}$ |
| $Q$ | volumetric spray flux | $m^3 \cdot s^{-1}$ |
| $q$ | surface heat flux | W |
| $q^*$ | dimensionless surface heat flux | |
| $RA$ | ratio of droplet cross-surface mean velocity and the volumetric spray flux | $m^{-2}$ |
| $Re$ | Reynolds number | |
| $T^*$ | dimensionless surface temperature | |
| $U_0, U_1, \ldots, U_5$ | droplet velocity at locations 0 to 5 shown in *figure 4* | $m \cdot s^{-1}$ |
| $\overline{u}$ | cross-surface mean droplet velocity | $m \cdot s^{-1}$ |
| $We$ | Weber number | |

*Greek symbols*

| | | |
|---|---|---|
| $\mu$ | viscosity | Pa·s |
| $\rho$ | density | $kg \cdot m^{-3}$ |
| $\sigma$ | surface tension | $N \cdot m^{-1}$ |

## 1. INTRODUCTION

Casting is the most economic industrial process used to transform liquid metals into near net shape components. Die casting is a commonly used technique in modern foundry industries in which the liquid metal is poured into the metal mould or squeezed into the mould under pressure. When a part comes out, it has the desired shape

* Correspondence and reprints.
gwliu@groupwise.swin.edu.au

for a particular application. In order to produce high quality castings, it is essential to understand the flow and heat transfer phenomena involved in the casting process.

There is a considerable body of open literature discussing the numerical modelling of the physical processes involved in casting processes. Most of it, however, is focused on the filling and solidification of liquid metal in the die. The modelling of these processes is normally based on finite difference or finite element methods and has reached a state of maturity. Currently there are many commercial software packages available in the market worldwide, such as MAVIS and DIANA (UK), SOLSTAR (USA), MAGMAsoft (Germany), Simulor (France) and Stefan Software (Japan). However, as far as spray cooling is concerned, none of these packages incorporate the mechanism of spray cooling.

In a high pressure die casting process, a liquid spray is used to lubricate as well as to cool the steel die. A thorough knowledge of the spray cooling of the die will facilitate the design and maintenance of a more thermally balanced die by the die caster, leading to improved quality and lower manufacturing costs. Despite the importance of die sprays in high pressure die casting, the heat removal characteristics of the die sprays are not well understood. As a result, there is no computer software available in the market which incorporates the total simulation of the spray cooling of the die. The work reported in this paper is the first step to rectify this.

A spray atomises bulk liquid into fine drops by either supplying liquid at high pressure through a small orifice (plain orifice spray) or by assisting liquid breakup using high pressure air (air-atomised spray). Significant heat transfer occurs when droplets produced by a liquid spray subsequently impact a hot surface.

As a metallic block is cooled by spray, its surface may experience four different heat transfer regimes: a film boiling regime, a transition boiling regime, a nucleate boiling regime and single-phase liquid cooling. The film boiling regime is characterised by an insulating vapour blanket on the surface which prevents the liquid from making direct contact with the surface and results in slow cooling. Once the temperature decreases below this point of minimum heat flux (the Leidenfrost point), the vapour blanket begins to collapse which ensures partial wetting of the surface. This transition boiling regime is marked by a significant increase in the surface heat flux owing to intense boiling, thus causing a rapid decrease in the surface temperature. The maximum heat flux occurs at the point of critical heat flux (CHF) where the vapour layer begins to vanish, causing the cooling rate to become a maximum. In the nucleate boiling regime, the entire surface experiences liquid contact and vigorous bubble production, keeping cooling rates fairly high. Boiling completely subsides in the single-phase cooling regime and the relatively low heat transfer rate is the result of convection. There has been no comprehensive model established for the heat transfer process during spray cooling because of the complexity of the mechanisms involved. Nevertheless, after conducting a review of literature on heat transfer to sprays in the film boiling regime, Brimacombe et al. [1] concluded that the volumetric spray flux has the greatest influence on the heat transfer coefficient.

Mudawar and Valentine [2] explored methods of determining the heat transfer coefficient of spray cooling to aluminium blocks in transition boiling, nucleate boiling, and single-phase cooling regimes using a plain orifice spray. They determined that the spray heat flux had to be based on the spray hydrodynamic parameters adjacent to the impingement location at the heater surface. Their heat transfer correlations were based on measurements made at the geometric centre of each spray. Deiters and Mudawar [3], and Mudawar and Deiters [4] later concluded that these correlations were valid at other locations within the spray field when the spray hydrodynamic parameters were determined for these locations.

Klinzing et al. [5] used the spray quenching heat transfer correlations and the spatial distribution models of the spray hydrodynamic parameters developed by Deiters and Mudawar [3, 6] to simulate the spray quenching of a thin, stationary rectangular Aluminium 1100 plate using the commercial finite element software package ANSYS. Subsequently, Mudawar and Deiters [4] predicted the temperature history of an Aluminium 1100 block which was sprayed over one surface and whose other surfaces were well insulated.

Yang et al. [7] studied the heat transfer phenomena in the nucleate boiling regime of spray cooling using air-driven spray nozzles and water as coolant. Flow field parameters such as liquid film thickness and flow rate were used to arrive at a correlation for the Nusselt number in the nucleate boiling regime.

The spray involved in a high pressure die casting process is air-atomised spray. Only a few research projects directly concerned with this process have been published. Altan et al. [8] investigated how various spraying parameters, especially the sprayed water/lubricant temperature and the spray pressure, affect the heat transfer from the die. They found that: (a) the temperature of the water in the spray tanks has little effect on the amount of heat removed from a heated die by spraying; (b) the depth of cooling by a water spray on dies is rather small. The die temperature, at 25 mm from the die surface, is relatively unaffected even by a spray of duration 3 seconds; (c) with the spray parameters commonly used in the die casting, the dies are below the Leidenfrost point, so boiling begins in the transition boiling regime. The critical heat flux occurs between surface temperatures of 165 °C and 215 °C. A quantitative relationship between the heat flux and the spray hydrodynamic parameters was not, however, established. Chhabra et al. [9], Lee et al. [10], Graff and Kallien [11] investigated experimentally the influences of different parameters such as air pressure, liquid flux density, die surface temperature and die lubricant composition on the die temperature and die surface heat flux. All these researchers did not achieve a quantitative relationship between the heat flux and the spray hydrodynamic parameters.

The aim of this paper is to examine the spray cooling mechanism involved in a high pressure die casting process using an experimental approach. The data obtained are then used to develop a new correlation to predict the spray heat flux quantitatively. To the authors' knowledge, this correlation will be the first quantitative equation to predict the spray cooling heat flux involved in a high pressure die casting process. Although other researchers such as Mudawar and Valentine [2] have developed correlations for spray cooling that were not applicable to high pressure die casting process.

## 2. EXPERIMENTAL SETUP

The experimental setup consists of a spray system, test heater, and a PDA spray droplet velocity and diameter measurement system.

### 2.1. Spray system

An air-atomised spray system was constructed and is shown schematically in *figure 1*. The spray nozzle was

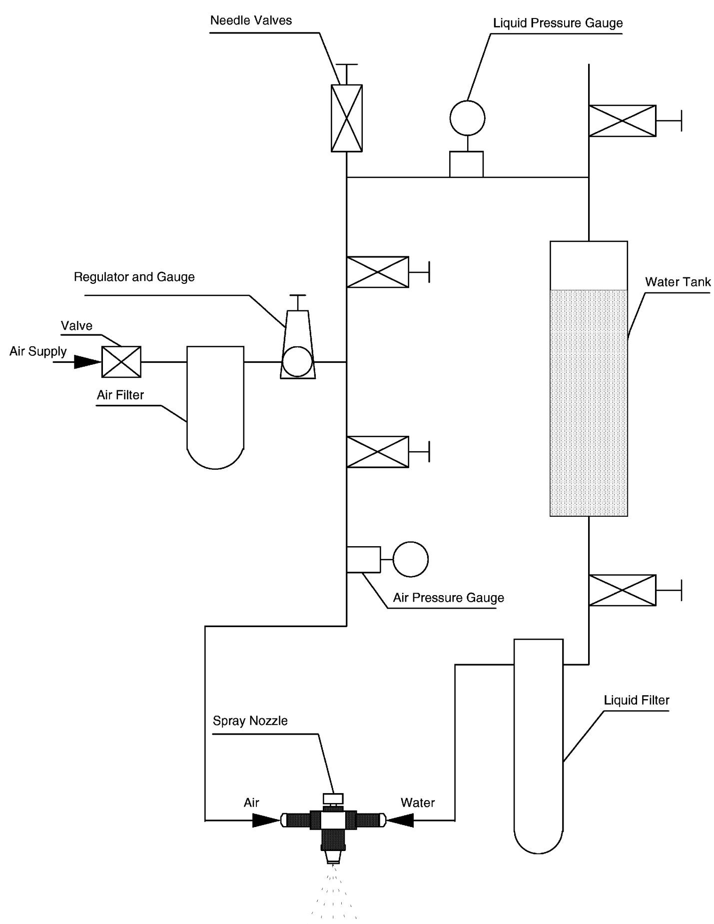


**Figure 1.** Schematic of the spray system.

supplied by Spraying System Co. Pty Ltd. The main air line supply was divided into two branches, one led directly to the air inlet of the spray nozzle and the other was used to pressurise water in the tank so that water could be supplied to the liquid inlet of the spray nozzle at any desired pressure. The main air line pressure could be regulated and measured by the air regulator and gauge. By careful regulation of the needle valves, the air pressure and liquid pressure to the nozzle can be adjusted independently to specified values. The pressurised liquid and compressed air were mixed internally to produce a completely atomised spray. Filters were also used to ensure the purity of the air and liquid components to the spray nozzle.

## 2.2. Test heater

The test heater was designed to investigate the local heat flux from the test-piece to the spray cooling. *Figure 2* shows the sectional view of the insulated test heater. In order to simulate the working conditions of a real die, the test-piece was made from H-13 steel. The tester operated in the range 150 °C to 350 °C which covered the range of initial die temperatures typically experienced in a die casting operation. The spray cooled surface area of the steel test-piece was small enough (10 mm diameter) to ensure that the whole surface was covered by the spray field. Heat was supplied to the test-piece by three 6 mm diameter cartridge heating elements which worked at a maximum temperature of 800 °C. Four high response K-type thermocouples were embedded in the neck of the sample to obtain temperature differentials. The corresponding temperature gradient obtained was then used to determine surface temperature and an estimation of surface heat flux using Fourier's law of heat conduction. A PC controlled Datataker, model DT50, manufactured by Data Electronics, was programmed to record the readings of all four thermocouples every half second.

The steel test heater was thermally insulated to reduce heat losses and to ensure that heat was conducted mainly to the spray cooled surface. The thermal insulation material used was Fibertex with a maximum service temperature of 650 °C and continuous service temperature of 550 °C, respectively. The test heater was well sealed with silicon sealant to prevent water from penetrating during spray cooling.

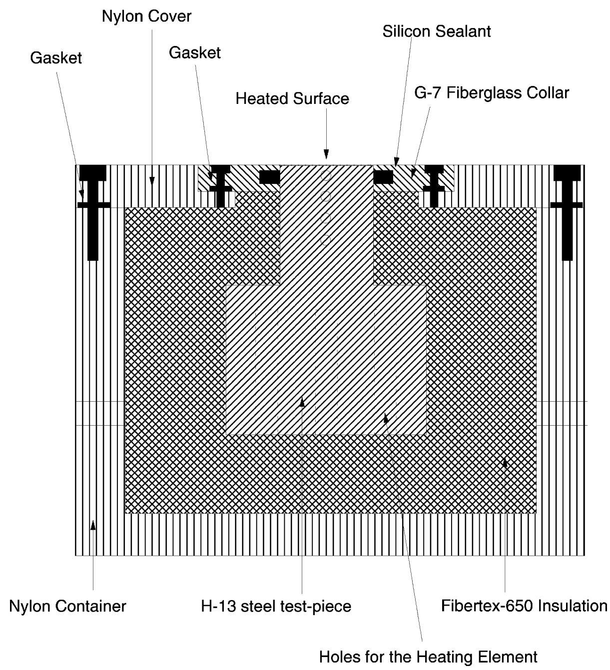


**Figure 2.** Sectional view of the insulated test heater.

## 2.3. PDA droplet velocity and diameter measurement

A Dantec Particle Dynamic Analyser (PDA) system [12, 13] was used to measure spray droplet size and velocity and their distributions simultaneously. *Figure 3* shows the schematic of the system.

A 4W argon ion laser was used to obtain a green beam (wave length of 514.5 nm). The transmitting optics consist of a collimator, polarisation rotator, a dispersion prism, a beam splitter, a Bragg cell, a beam spacer and a fiber optic module with a 150 mm focal length lens. In setting up the transmitting optics, attention was paid to such factors as mode structure, polarisation, optical path length balancing and correct beam waist positioning in the measurement volume. A frequency shift of 40 MHz was introduced in one of the crossing laser beams to overcome the sign ambiguity of the velocity measurements.

The time mean velocity and the Sauter mean diameter of the droplet were calculated using the following equations:

$$U = \frac{\sum_{i=1}^{N} U_i \, \Delta t_i}{\sum_{i=1}^{N} \Delta t_i}$$

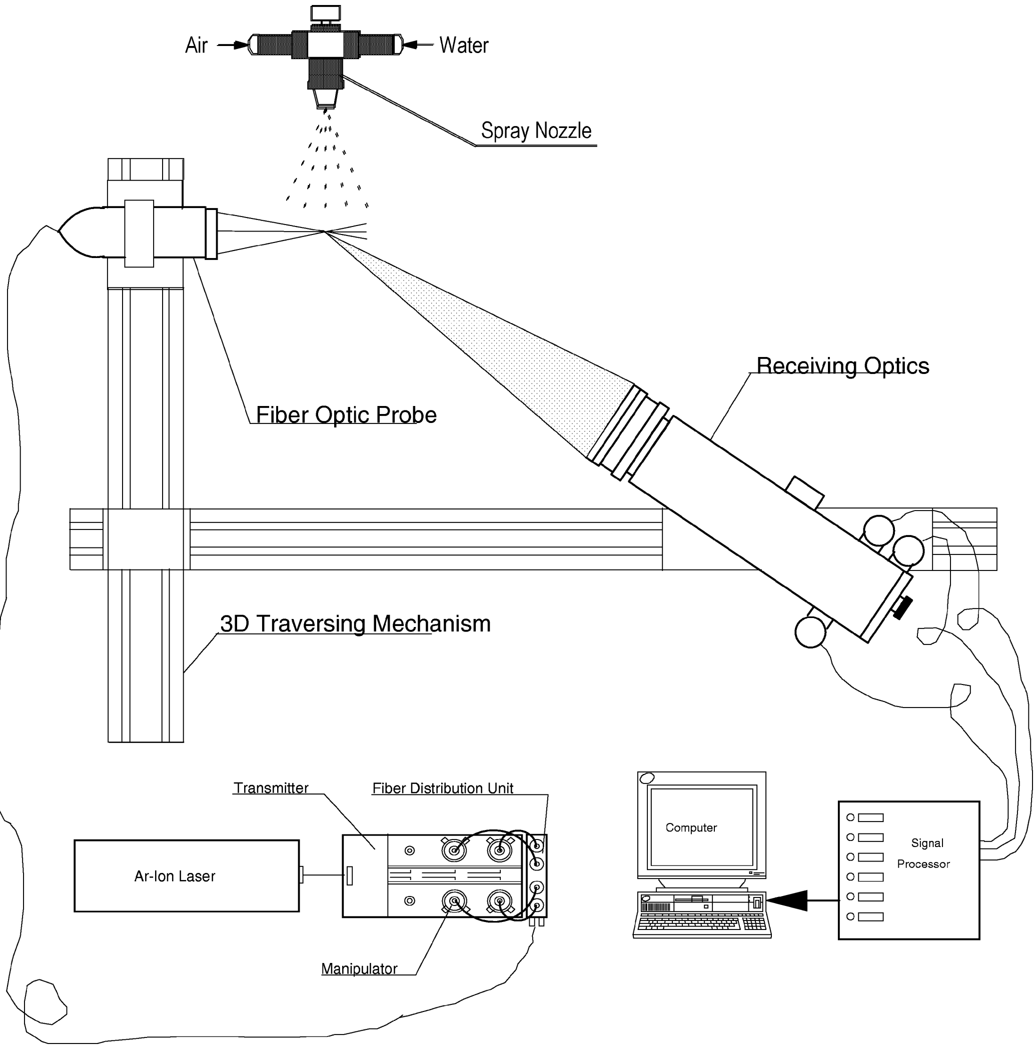


**Figure 3.** Schematic of the PDA system.

$$D_{32} = \frac{\sum_{i=1}^{N} D_i^3}{\sum_{i=1}^{N} D_i^2}$$

in which $U$ is the time mean axial velocity, $D$ is the diameter of particle, $D_{32}$ is the Sauter mean diameter, the subscript $i$ denotes the $i$th particle, $N$ is the number of particles (sample size), and $\Delta t_i$ is the transit time of the $i$th particle for residence time weighting.

## 3. EXPERIMENTAL PROCEDURE

At the beginning of each test the water tank was filled with fresh water. Power was then supplied to the heating elements to bring the surface temperature of the test heater to around 350 °C. The insulated test heater was then positioned at the center of the spray field 30 mm below the spray nozzle. The air pressure and the water pressure to the nozzle were then adjusted until the desired pressure was obtained and then spray was applied to the hot surface of the test heater. Readings of the all four thermocouples were recorded every 0.5 s during spray cooling and the recorded data were saved as a data matrix.

The volumetric liquid spray flux, that is the liquid flow rate per unit surface area, was then measured. The test heater was removed and a cylinder of 10 mm internal

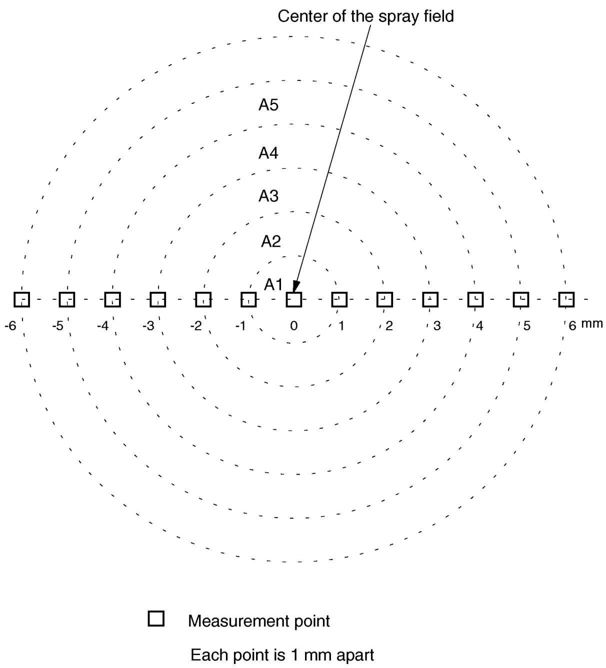


**Figure 4.** Locations of droplet velocity and diameter measurement points used in the experiment.

diameter was placed into the spray field so that the cylinder inlet was at the same location as the test heater. The time to fill a prescribed volume of water in the cylinder was measured from which the liquid spray flux was calculated.

The PDA system was used to determine the hydrodynamic parameters of the spray including droplet velocity and diameter. The intersection of the two laser beams was located at a distance of 30 mm below the spray nozzle where the spray droplets impinge on the hot surface. A 3D traversing mechanism was used to measure the droplet velocity and diameter distribution across the spray field. *Figure 4* shows the locations of the measurement points used in the experiment.

## 4. EXPERIMENTAL UNCERTAINTY

Measuring frequency of the PDA bursts, which depends primarily on laser wave length and the beam crossing angle, can introduce some errors. The beam crossing angle may introduce some uncertainty in the measured velocity although the error associated with the wave length for an argon ion laser is generally negligible. The beam spacing of 38 mm used in this study was assumed to have an error of ±0.5 mm, which can introduce

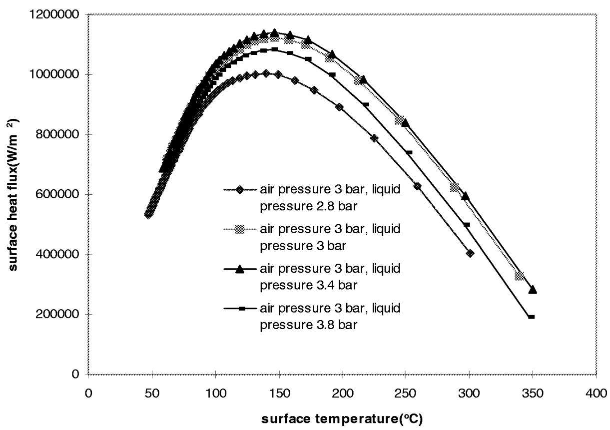


**Figure 5.** Measured surface heat flux for fixed air pressure and various liquid pressures.

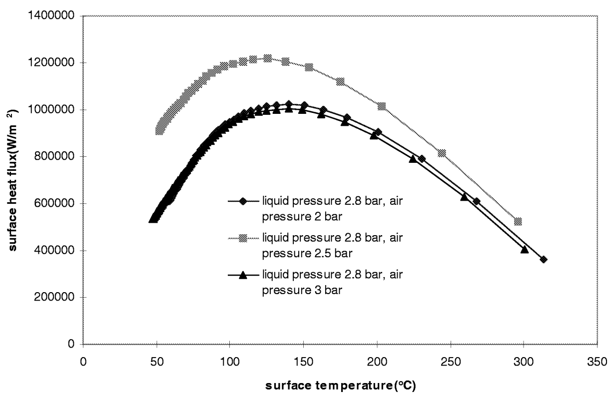


**Figure 6.** Measured surface heat flux for fixed liquid pressure and various air pressures.

an uncertainty in the measured velocity of 1 %. However, it should be stated that the error arising from the uncertainty of the optical configuration is constant and affects all measurements equally.

## 5. EXPERIMENTAL RESULTS AND DISCUSSION

### 5.1. Heat transfer

*Figures 5–7* show the measured surface heat flux at different conditions. All these data were used to develop the correct correlation for predicting spray cooling heat flux as discussed in the next section.

From *figure 5*, it is noted that at a constant air pressure of 3 bar, the heat flux keeps increasing when

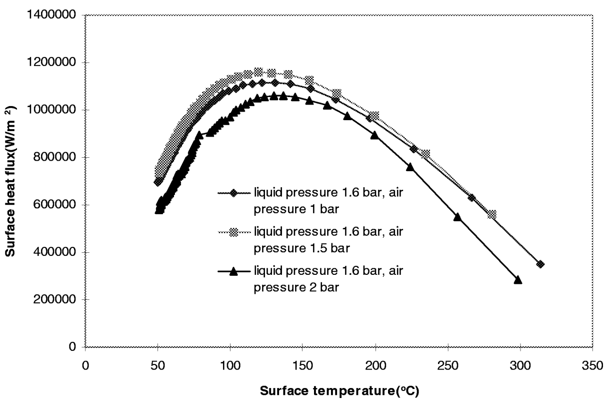


**Figure 7.** Measured surface heat flux for fixed liquid pressure and various air pressures.

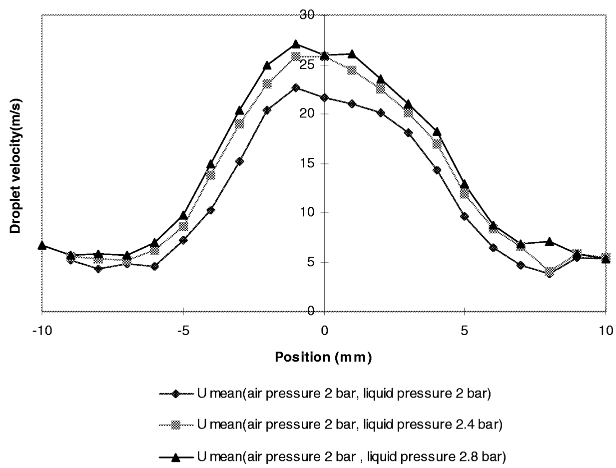


**Figure 8.** $U$-mean distribution for fixed air pressure and various liquid pressures.

liquid pressure increases from 2.8 bar to 3.4 bar at a given temperature over the temperature range. At further increase of the liquid pressure from 3.4 bar to 3.8 bar, the heat flux decreases. An increase of liquid pressure combined with a constant air pressure results in increases of the volumetric spray flux, the droplet velocity and the droplet diameter. The behavior of the heat flux depends on the combined effects of all these parameters. *Figures 6* and *7* reveal that at constant liquid pressure, the heat flux first increases with the increase of air pressure, and then decreases with the further increase of air pressure. At a constant liquid pressure, the volumetric spray flux and droplet diameter decrease with the increase of air pressure. The decrease of the volumetric spray flux tends to reduce the heat flux. However, the decrease of droplet diameter will improve the heat transfer. The effects of these two parameters makes the heat flux first increase with the air pressure at a given liquid pressure, and then decrease with further increase of air pressure.

*Figures 5–7* also reveal that the critical heat flux (the maximum heat flux shown in all the curves) occurs in the temperature range of 125–150 °C during spray cooling involved in high pressure die casting process.

## 5.2. Hydrodynamic parameters of the spray

The droplet mean velocity distribution when the air pressure is fixed at 2 bar and the liquid pressure varies from 2 bar to 2.8 bar is shown in *figure 8*. As expected, for a given air pressure, the increase of liquid pressure increases the droplet velocity. *Figure 9* shows the droplet

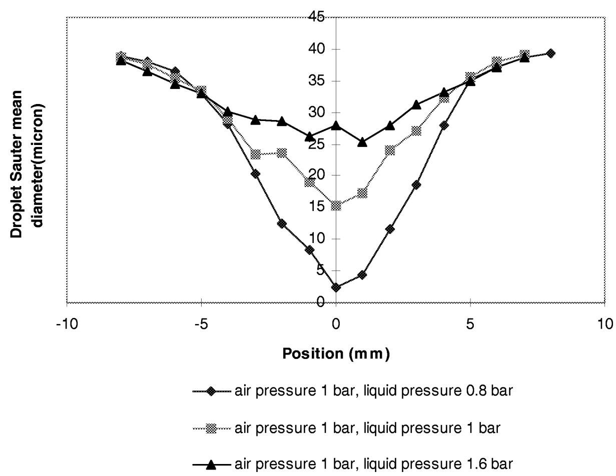


**Figure 9.** Influence of liquid pressure on droplet size when air pressure is constant.

Sauter mean diameter profile at a given air pressure and various liquid pressures. The droplet Sauter mean diameter increases with the increase of liquid pressure. The droplet Sauter mean diameter profile at constant liquid pressure and various air pressures is shown in *figure 10*. The droplet Sauter mean diameter decreases with the increase of air pressure.

*Figures 8–10* also show that both the spray droplet velocity and diameter vary across the surface cooled by the spray. To characterize the spray droplet velocity and diameter adjacent to the surface, the cross-surface mean droplet velocity and diameter were defined and calculated as follows.

Cross-surface mean velocity:

$$\overline{u} = \left\{ \frac{1}{2}(U_0+U_1)A_1 + \frac{1}{2}(U_1+U_2)A_2 + \frac{1}{2}(U_2+U_3)A_3 + \frac{1}{2}(U_3+U_4)A_4 + \frac{1}{2}(U_4+U_5)A_5 \right\} \cdot (A_1+A_2+A_3+A_4+A_5)^{-1} \quad (1)$$

Cross-surface Sauter mean diameter:

$$\overline{d} = \left\{ \frac{1}{2}(d_0+d_1)A_1 + \frac{1}{2}(d_1+d_2)A_2 + \frac{1}{2}(d_2+d_3)A_3 + \frac{1}{2}(d_3+d_4)A_4 + \frac{1}{2}(d_4+d_5)A_5 \right\} \cdot (A_1+A_2+A_3+A_4+A_5)^{-1} \quad (2)$$

where $A_1$–$A_5$ are the ring areas, $U_0$–$U_5$ are the measured velocities at locations 0–5, and $d_0$–$d_5$ are the measured droplet Sauter mean diameters at locations 0–5 shown in *figure 4*.

*Table I* shows the cross-surface-mean droplet velocity, cross-surface-mean Sauter mean droplet diameter, and the measured volumetric spray flux at different spray conditions. All these values are essential for developing the correlation discussed in the next section.

## 6. CORRELATION DEVELOPMENT

The parameters that were considered important in influencing the spray cooling heat flux are the following:

$$q = f\left(Q, d, \overline{u}, \sigma, T_{\mathrm{sur}}, h_{\mathrm{fg}}, \rho, C_{\mathrm{pl}}, \mu\right) \quad (3)$$

Dimensional analysis was carried out using the Buckingham PI method [14–16]. The following dimensionless groups were formed:

$$\frac{q}{\rho Q h_{\mathrm{fg}}}, \quad \frac{\rho \overline{u}\overline{d}}{\mu}, \quad \frac{\sigma}{\rho \overline{u}^2 \overline{d}}, \quad \frac{T_{\mathrm{sur}} C_{\mathrm{pl}}}{h_{\mathrm{fg}}}, \quad \frac{\overline{u}}{Q}$$

We define:

$$q^* = \frac{q}{\rho Q h_{\mathrm{fg}}} \quad \text{dimensionless heat flux}$$

$$T^* = \frac{T_{\mathrm{sur}} C_{\mathrm{pl}}}{h_{\mathrm{fg}}} \quad \text{dimensionless surface temperature}$$

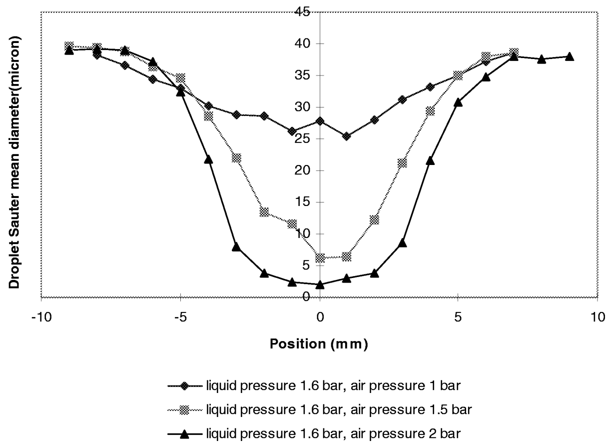


**Figure 10.** Influence of air pressure on droplet size when liquid pressure is constant.

TABLE I
The cross-surface-mean droplet velocity, cross-surface-mean Sauter mean droplet diameter, and the volumetric spray flux at different spray conditions.

| Air pressure (bar) | Liquid pressure (bar) | Cross-surface mean velocity $\overline{u}$ ($\mathrm{m \cdot s^{-1}}$) | Cross-surface Sauter mean diameter $\overline{d}$ (μm) | Volumetric spray flux ($\mathrm{m^3 \cdot s^{-1}}$) |
|---|---|---|---|---|
| 1 | 0.8 | 14.0896 | 22.3 | 0.006789 |
| 1 | 1 | 14.98828 | 27.6 | 0.008632 |
| 1 | 1.2 | 15.8463 | 30.7 | 0.01232 |
| 1 | 1.6 | 18.68805 | 30.6 | 0.01712 |
| 2 | 1.6 | 14.47558 | 9.21 | 0.006621 |
| 2 | 2 | 14.85058 | 12.5 | 0.009938 |
| 2 | 2.4 | 17.62382 | 15.8 | 0.01319 |
| 2 | 2.8 | 18.832 | 16.2 | 0.01598 |
| 3 | 2.8 | 14.41416 | 4.23 | 0.006482 |
| 3 | 3 | 15.23197 | 6.62 | 0.008482 |
| 3 | 3.4 | 17.8983 | 6.84 | 0.01163 |
| 3 | 3.8 | 18.82802 | 8.23 | 0.014973 |

$$Re = \frac{\rho \overline{u}\overline{d}}{\mu} \quad \text{Reynolds number}$$

$$We = \frac{\sigma}{\rho \overline{u}^2 \overline{d}} \quad \text{Weber number}$$

$$RA = \frac{\overline{u}}{Q} \quad \text{the ratio of the droplet velocity and the volumetric liquid flux}$$

Then, we have

$$q^* = f(Re, We, T^*, RA) \tag{4}$$

At each experimental case, *Re*, *We*, and *RA* are constant, $q^*$ is only a function of the dimensionless surface temperature $T^*$. For each test case, it was found that quite accurate relationships between $q^*$ and $T^*$ could be established by the following polynomial:

$$q^* = AT^{*3} + BT^{*2} + CT^* + D \tag{5}$$

in which each of the coefficients $A$, $B$, $C$, $D$ differs for each test case and are clearly functions of *Re*, *We*, and *RA*.

Least squares fitting of $A$, $B$, $C$, $D$ values to the values of *Re*, *We*, and *RA* for the experimental data resulted in the following equations:

$$A = 10^{-4.05434} Re^{1.45101} We^{1.27899} RA^{0.864281} \tag{6}$$

$$B = -10^{-3.6164} Re^{1.31859} We^{1.17256} RA^{0.915949} \tag{7}$$

$$C = 10^{-3.64182} Re^{1.21498} We^{1.09276} RA^{0.949317} \tag{8}$$

$$D = -10^{-4.15201} Re^{1.13977} We^{1.03674} RA^{0.963274} \tag{9}$$

Equation (5) is the proposed correlation to predict the spray cooling heat flux involved in a high pressure die casting process with the coefficients defined in equations (6)–(9). This correlation is capable of predicting the heat flux at all the heat transfer regimes involved in the spray cooling of a high pressure die casting process.

## 7. EVALUATION OF THE EMPIRICAL CORRELATION

To validate the correlation equation (5), comparison was made with the previously discussed experimental data. As shown in *figures 11* and *12*, the correlation prediction is in satisfactory agreement with the experimental data. This correlation is only suitable for predicting the spray cooling heat flux involved in a high pressure die casting process with water as coolant.

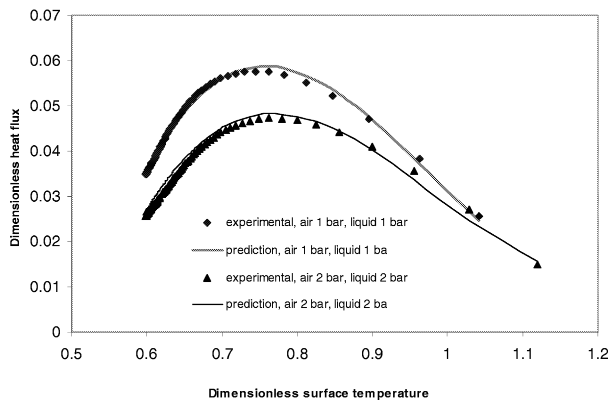


**Figure 11.** Comparison between the prediction and the experimental data at air pressure and liquid pressure both at 1 bar and both at 2 bar.

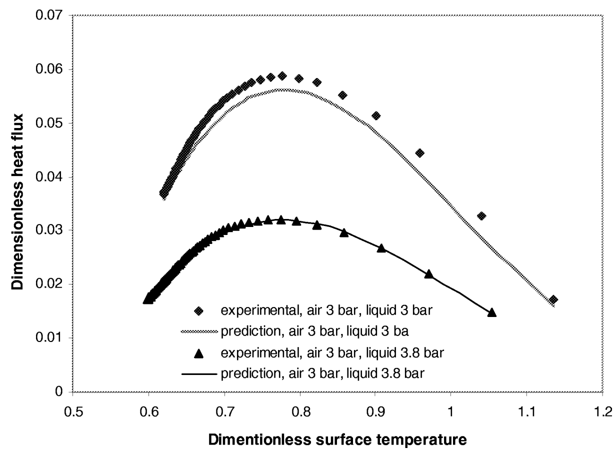


**Figure 12.** Comparison between the prediction and the experimental data at air pressure 3 bar, liquid pressure 3 bar and 3.8 bar.

## 8. CONCLUSION

An empirical correlation that relates the spray cooling heat flux to the spray hydrodynamic parameters was developed. This correlation can be used to predict spray cooling heat flux involved in a high pressure die casting process with water as coolant. The agreement between the prediction and the experimental data is satisfactory. The proposed correlation can be used to develop a more accurate prediction of the cooling process in commercial software packages such as MAGMAsoft.

### *Acknowledgements*

Financial support of this work by a grant from Australian Research Council is gratefully acknowledged. The authors would like to thank Dr. J.P. van der Walt, Dr. William Yang of our research group, and Dr. N.J. Lawson of the University of Melbourne for their help and valuable discussions.

## REFERENCES

[1] Brimacombe J.K., Agarwal P.K., Baptista L.A., Hibbins S., Prabhakar B., Spraying cooling in the continuous casting of steel, in: 63rd National Open Hearth and Basic Oxygen Steel Conf. Proc., Vol. 63, 1980, pp. 235–252.

[2] Mudawar I., Valentine W.S., Determination of the local quenching curve for spary-cooled metallic surfaces, J. Heat Treat. 7 (1989) 107–121.

[3] Deiters T.A., Mudawar I., Prediction of the temperature–time cooling curves for three-dimensional aluminium products during spray quenching, J. Heat Treat. 8 (1990) 81–91.

[4] Mudawar I., Deiters T.A., A universal approach to predicting temperature response of metallic parts to spray quenching, Int. J. Heat Mass Tran. 37 (1994) 347–362.

[5] Klinzing W.P., Rozzi J.C., Mudawar I., Film and transition boiling correlations for quenching of hot surface with water sprays, J. Heat Treat. 9 (1992) 91–103.

[6] Deiters T.A., Mudawar I., Optimisation of spray quenching for aluminium extrusion, forging, or continuous casting, J. Heat Treat. 7 (1989) 9–18.

[7] Yang J., Chow L.C., Pais M.R., Nucleate boiling heat transfer in spray cooling, J. Heat Tran. 118 (1996) 668–671.

[8] Altan T., Bishop S.A., Miller R.A., Chu Y.L., A preliminary investigation on the cooling and lubrication of die casting dies by spraying, in: NADCA, Detroit-T91-115, 1991, pp. 355–361.

[9] Chhabra S., Chu Y.L., Altan T., An investigation of cooling and lubrication of die casting dies using a water/lubricant spray, Die Casting Engineer (January/February 1993) 24–27.

[10] Lee I.S., Nguyen T.T., Leigh G.M., Cooling effect of lubricant sprays on die casting dies, in: NADCA, Detroit-T91-111, 1991, pp. 329–334.

[11] Graff J., Kallien L.H., The effect of die lubricant spray on the thermal balance of dies, in: NADCA, Cleveland-T93-083, 1993, pp. 239–246.

[12] Dantec PDA User's Manual, 1992.

[13] Drain L.E., The Laser Doppler Technique, Wiley, 1980.

[14] Daugherty R.L. et al., Fluid Mechanics with Engineering Applications, McGraw-Hill, 1989, Chapter 7.

[15] Roberson J.A., Crowe C.T., Engineering Fluid Mechanics, 6th edition, Wiley, 1997, Chapter 8.

[16] Langhaar H.L., Dimensional Analysis and Theory of Models, Wiley, 1951.